Biotin-Streptavidin Sensitive BioFETs and Their Properties

Thomas Windbacher, Viktor Sverdlov, and Siegfried Selberherr

Institute for Microelectronics, TU Wien, Gußhaustraße 27–29/E360, A-1040, Wien, Austria
{Windbacher,Sverdlov,Selberherr}@iue.tuwien.ac.at

Abstract. In this work the properties of a biotin-streptavidin BioFET have been studied numerically with homogenized boundary interface conditions as the link between the oxide of the FET and the analyte which contains the bio-sample. The biotin-streptavidin reaction pair is used in purification and detection of various biomolecules; the strong streptavidin-biotin bond can also be used to attach biomolecules to one another or onto a solid support. Thus this reaction pair in combination with a FET as the transducer is a powerful setup enabling the detection of a wide variety of molecules with many advantages that stem from the FET, like no labeling, no need of expensive read-out devices, the possibility to put the signal amplification and analysis on the same chip, and outdoor usage without the necessity of a lab.

1 Introduction

Today's technology for detecting tumor markers, antigen-antibody complexes, and pathogens is time-consuming, complex, and expensive [1, 2]. For instance, a typical procedure to detect a given DNA complex is to increase the concentration by Reverse Transcription (RT) or Polymerase Chain Reaction (PCR), followed by a process step that will add a label to the DNA enabling detection by light or radiation. After all these steps the sample is applied to a microarray. The microarray consists of an array of spots, and every single spot is able to detect a different type of molecule. After the reaction has taken place the array is read by an expensive microarray reader.

Replacing the above sensing mechanism by electrical detection has several benefits. First, the optical microarray reader becomes superfluous. Detection by FET (field-effect transistor) makes the integration of amplifying and analyzing circuits on the same chip possible, thus saving also equipment. The advanced development of semiconductor process technology allows mass production of such devices, decreasing the price dramatically. Various kinds of reaction pairs are possible and have been studied, like detection of DNA [3,4,5,6,7], cancer markers [8], proteins, e.g. biotin-streptavidin [9,10,11,12], albumin [13], and transferrin [14]. In principle, every molecule which is charged in the solute and which can be bound to the surface layer can be detected by a BioFET. The field of applications is very wide and spans from DNA sequencing and point of care applications to controlling environmental pollution and the spread of diseases. The BioFET can be easily integrated into the chip environment. By putting a microfluidic channel above the functionalized gate of the BioFET the chip can be turned into a mini-laboratory - the lab-on-chip. This enables better control of the environmental parameters (e.g. local pH or detecting the amount of a special protein) and gives the possibility

A. Fred, J. Filipe, and H. Gamboa (Eds.): BIOSTEC 2009, CCIS 52, pp. 85–95, 2010.

of local measurement (e.g. how a cell reacts to a stimulus), thus providing a complete lab-on-a-chip.

2 Method

A BioFET consists of several parts: a semiconductor transducer, a dielectric layer, a biofunctionalized surface, and the analyte (Figure 1). The semiconductor transducer is a conventional FET. The dielectric layer is the gate oxide, and the biofunctionalized surface contains immobilized biomolecule receptors attached, so it is able to bind the desired molecule. The analyte is in an aqueous solution. If a target molecule binds to a receptor, the local charge density at the surface changes and thus the potential in the semiconductor and so the conductivity of the channel of the field-effect transducer is changed.

The binding of the target with the receptor happens at the Angstrom length scale, while the semiconductor device is in the micrometer length scale. Thus a proper way of describing the semiconductor-solution interface is crucial.

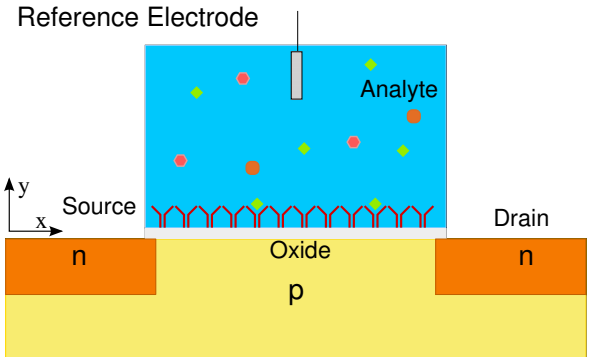

Fig. 1. Schematic diagram of a BioFET.

Transport in a FET with a gate length of $1\mu\mathrm{m}$, can be modeled via the drift-diffusion approach [15, 16]. The aqueous solution is described by the Poisson-Boltzmann equation.

$$\epsilon_0 \nabla \cdot (\epsilon_{\mathrm{Ana}} \nabla \psi(x,y)) = -\sum_{\sigma \in S} \sigma \; q \; c_\sigma^\infty \; e^{-\sigma \frac{q}{k_\mathrm{B} T}(\psi(x,y)-\psi_\mu)} \tag{1}$$

k_B denotes Boltzmann's constant, T the temperature in Kelvin, and σ the indices out of the set S containing the valences of the ions in the electrolyte. ϵ_0 describes the permittivity of vacuum, and q the elementary charge. ψ_μ is the chemical potential. c_σ^∞ is the bulk ion concentration in equilibrium, while $\epsilon_{\mathrm{Ana}} \approx 80$ is the relative permittivity of water.

The sum describes the carrier densities arising from the Boltzmann model. Assuming sodium-chloride as salt, which is a $1:1$ salt, the expression given in (1) can be reduced to

$$\epsilon_0 \nabla \cdot (\epsilon_{\mathrm{Ana}} \nabla \psi(x,y)) = 2q \; c_\sigma^\infty \; \sinh\left(\frac{q}{k_\mathrm{B} T}(\psi(x,y) - \psi_\mu)\right) \; . \tag{2}$$

The charge on the surface due to chemical reaction of the H^+ and OH^- has been modeled at $pH = 7$ with the site-binding model [2]:

$$Q_{\mathrm{Ox}} = q\, N_{\mathrm{S}}\, \frac{\frac{[H^+]_{\mathrm{b}}}{\mathrm{K_a}}\, e^{-\frac{q}{k_{\mathrm{B}}T}\Psi(x,y)} - \frac{\mathrm{K_b}}{[H^+]_{\mathrm{b}}}\, e^{\frac{q}{k_{\mathrm{B}}T}\Psi(x,y)}}{1 + \frac{[H^+]_{\mathrm{b}}}{\mathrm{K_a}}\, e^{-\frac{q}{k_{\mathrm{B}}T}\Psi(x,y)} + \frac{\mathrm{K_b}}{[H^+]_{\mathrm{b}}}\, e^{\frac{q}{k_{\mathrm{B}}T}\Psi(x,y)}}\ . \tag{3}$$

N_{S} denotes the surface binding site density, while $\mathrm{K_a}$ and $\mathrm{K_b}$ are the equilibrium constants for charging the surface positively and negatively, respectively. $[H^+]_{\mathrm{b}}$ describes the positive hydrogen ion concentration of the bulk and is corrected to the activity of the hydrogen concentration by the $e^{\frac{q}{k_{\mathrm{B}}T}\Psi(x,y)}$ terms.

The biomolecules are modeled in a physics-based bottom-up approach. By calculating the charge and dipole moment for a single molecule (see for example Figure 2, [17]), a mean charge density and a mean dipole moment density of the boundary layer is obtained. This bridges the gap between the Angstrom length scale of the biomolecules and the micrometer dimensions of the FET [18, 19, 20, 21].

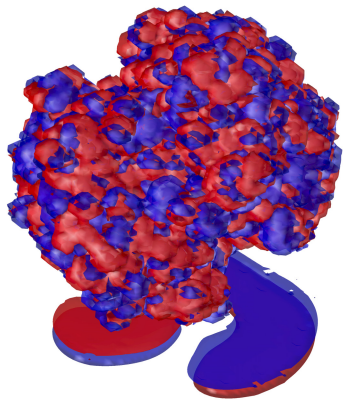

Fig. 2. Biotin-streptavidin complex [22] on the oxide surface. Two iso-surfaces for plus and minus $0.1\ \frac{k_{\mathrm{B}}T}{qA^2}$ are shown.

The link between the gate oxide and the aqueous solution is realized by two interface conditions, [18, 19, 23],

$$\epsilon_0\epsilon_{\mathrm{Oxid}}\ \partial_y\psi(0-,x) - \epsilon_0\epsilon_{\mathrm{Ana}}\ \partial_y\psi(0+,x) = -C(x), \tag{4}$$

$$\psi(0-,x) - \psi(0+,x) = -\frac{D_y(x)}{\epsilon_{\mathrm{Ana}}\epsilon_0}\ . \tag{5}$$

The x-axis is parallel oriented to the oxide surface, while the y-axis points into the liquid. $\psi(0-)$ describes the potential in the oxide, while $\psi(0+)$ relates to the potential in the solute. The first equation describes the jump in the field, while the second introduces a dipole moment which causes a shift of the potential taken into account by adjusting the potential in the analyte (Figure 3).

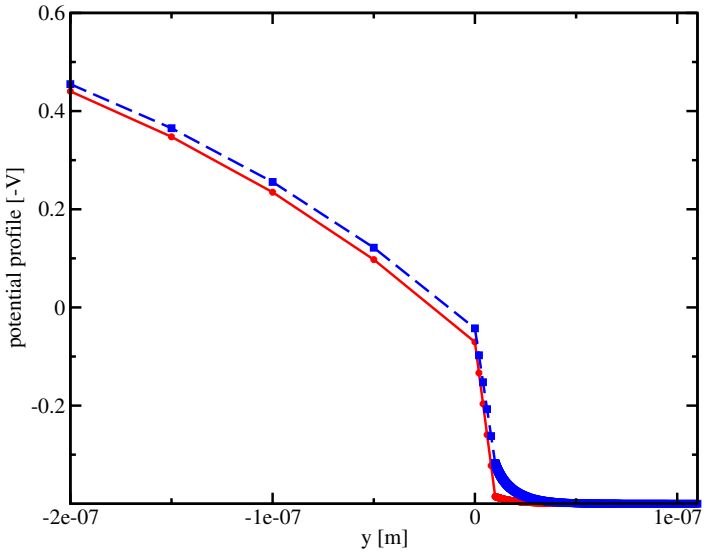

Fig. 3. Potential profile at the interface (from left to right: semiconductor, oxide, solute). The dashed line shows the profile, when biotin and streptavidin are attached to the surface (for10 nm density), while the full line shows the potential with water and salt only.

3 Simulation

Three different types of dielectric were simulated. SiO_2 as a reference, Al_2O_3, and Ta_2O_5 as possible high-k materials, with relative permitivities of 3.9, 10, and 25, respectively. As solute 1 mMol sodium-chloride at $pH = 7$ was considered. The parameters for the site-binding model can be found in Table 1 [24]. For each dielectric the unprepared state (just water and salt), the prepared state (water, salt, and biotin), and the bound state, when the chemical reaction has taken place (water, salt, and biotin-streptavidin), were calculated for two different mean distances between molecules ($\lambda = 10\,\mathrm{nm}$, $\lambda = 15\,\mathrm{nm}$). The data used for calculating charge and dipole moment of biotin and streptavidin are obtained from `http://www.pdb.org/` (Figure 2, Figure 11, [25]). The potential distribution across the device is shown in Figure 4 and output curves were calculated for every parameter combination mentioned above, assuming a 100% binding efficency. The potential of the reference electrode is set to $0.4\,\mathrm{V}$ so that the FET will be in moderate inversion as proposed by [26].

Table 1. The parameters needed for the site-binding model using different dielectric

Oxide	pK_a	pK_b	$N_S\ [cm^{-2}]$	Reference
SiO_2	-2	6	$5 \cdot 10^{14}$	[27]
Al_2O_3	6	10	$8 \cdot 10^{14}$	[27]
Ta_2O_5	2	4	$10 \cdot 10^{14}$	[28]

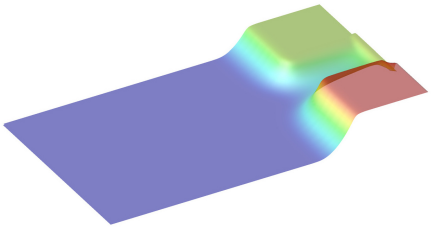

Fig. 4. Potential profile for Ta_2O_5 water, salt, and biotin-streptavidin at $\lambda = 10\,\mathrm{nm}$ average distance. Blue denotes $-1\,\mathrm{V}$ while red stands for $1\,\mathrm{V}$.

4 Results

Figures 5, 6, and 7 show a decrease in the output current for biotin attached to the surface in comparison to the unprepared surface. This downward shift for the bound state in comparison to the unbound state is due to the increase of negative charges at the interface, which is also confirmed by the difference between the curves for $\lambda = 10\,\mathrm{nm}$ and $\lambda = 15\,\mathrm{nm}$, since for $10\,\mathrm{nm}$ the molecules are located denser than for $15\,\mathrm{nm}$.

As can be seen in the Figures 5, 6, and 7, the bigger the ϵ_r of the dielectric the bigger is the output current. Thus high-k materials deliver stronger output signals. According to [29] however, higher ϵ_r dielectric constants may lead to higher trap densities and thus

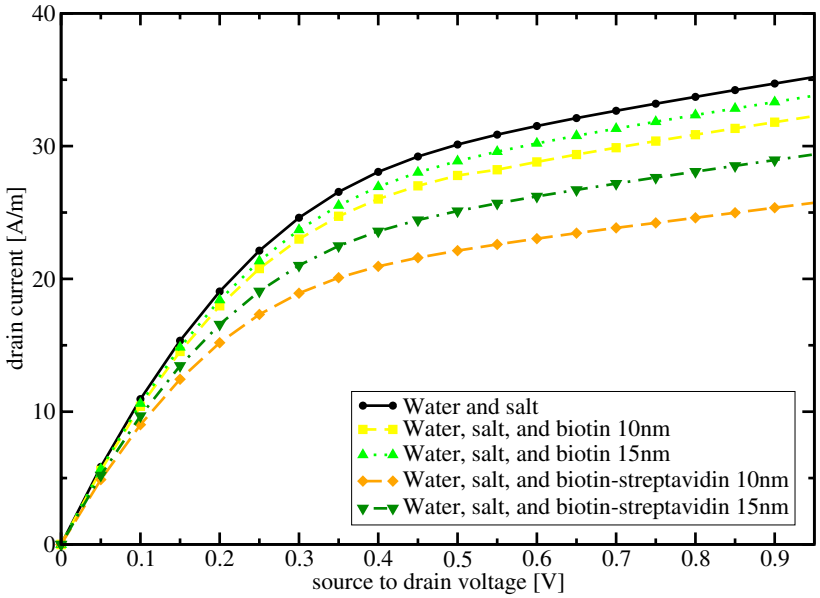

Fig. 5. Output curve for SiO_2 for unprepared, prepared but unbound, and bound state at $\lambda = 10\,\mathrm{nm}$ and $\lambda = 15\,\mathrm{nm}$, respectively.

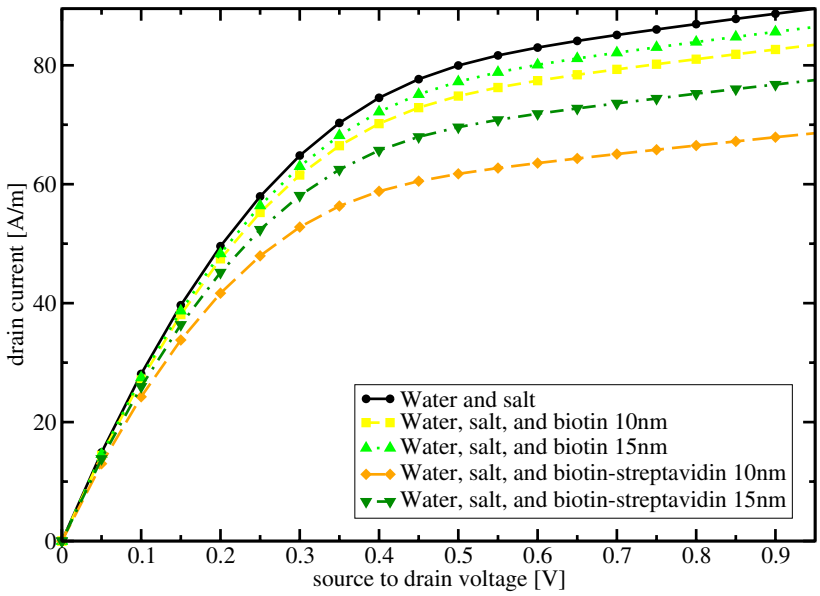

Fig. 6. Output curve for Al_2O_3 for unprepared, prepared but unbound, and bound state at $\lambda = 10\,\mathrm{nm}$ and $\lambda = 15\,\mathrm{nm}$, respectively.

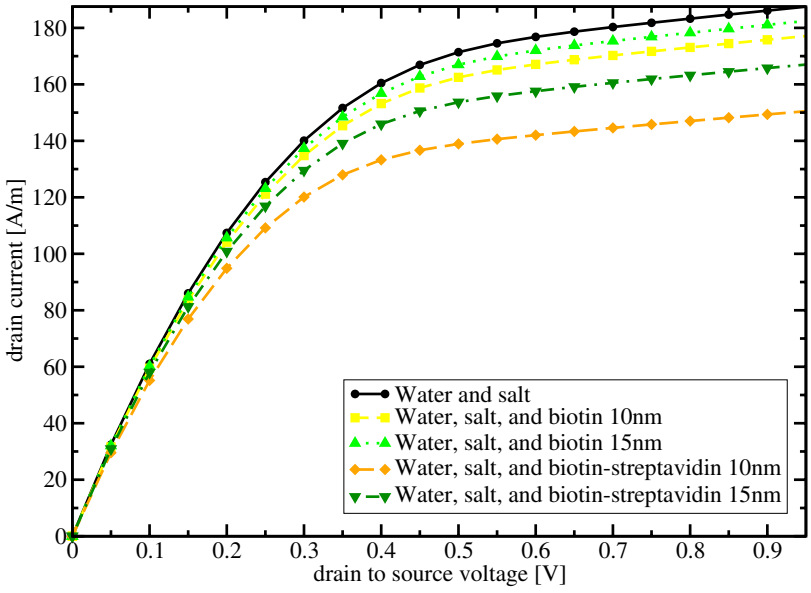

Fig. 7. Output curve for Ta_2O_5 for unprepared, prepared but unbound, and bound state at $\lambda = 10\,\mathrm{nm}$ and $\lambda = 15\,\mathrm{nm}$, respectively.

to a decreased signal-to-noise ratio. Therefore, a trade-off between bigger output signal and signal-to-noise ratio has to be met.

Figure 8 shows the output curves as a function of dielectric and molecule orientation (0° means perpendicular to the surface and 90° means lying flatly on the surface) leading to the lowest output curves for 0° followed by 90° and the curves without dipole moment for each group. Figures 9 and 10 show the small signal or differential resistance as a function of dielectric and molecule orientation, displaying smaller values for higher relative permittivity ϵ_r. A slightly larger differential resistance is observed for perpendicular molecule orientation, in agreement with the previous results shown in Figures 5, 6, and 7. This is expected, because biomolecules are inhomogeneously charged. Therefore, they possess a dipole moment which enters into the boundary conditions (5) and there should be a difference in the output curves of the BioFET for different orientation angles in relation to the surface.

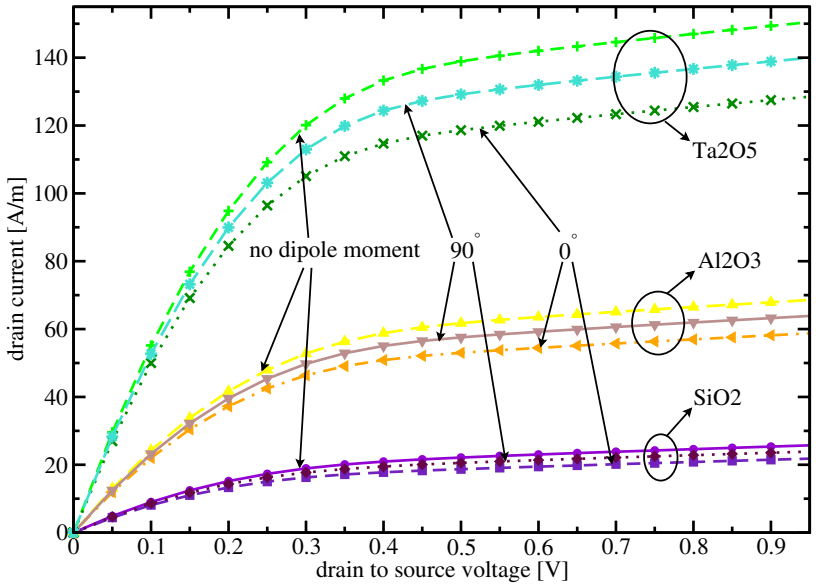

Fig. 8. Output curves for SiO_2, Al_2O_3, and Ta_2O_5 for calculation without dipole moment, angle 0° (perpendicular to surface), and angle 90° (parallel to surface).

In the biochemical community there is an ongoing discussion, if the orientation of the biomolecule is relevant for sensing. Several papers have shown contradictory results [30,31,32,33,34]. All these papers are based on optical detection. Although more study is needed, we mention that for optical detection it is more important to choose the linking molecule in a way that the reaction is not hindered by steric effects (receptors block each other) or the binding sites are blocked or even broken by the crosslinker. In the case of a BioFET, however, a field-effect as working principle is used. Thus it is important to have a linker which is as short as possible, to be close to the surface.

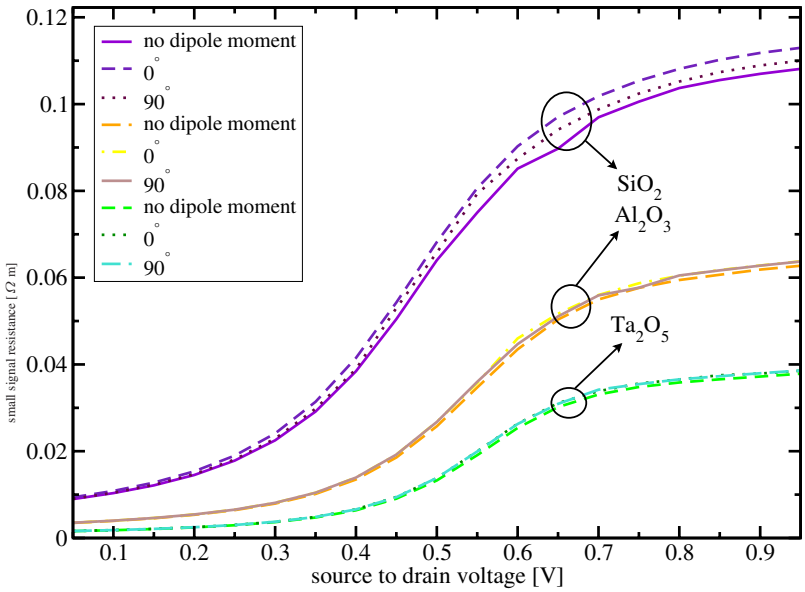

Fig. 9. Small signal resistance for SiO_2, Al_2O_3, and Ta_2O_5 calculated without dipole moment, angle $0°$ (perpendicular to surface), and angle $90°$ (parallel to surface) at biotin only.

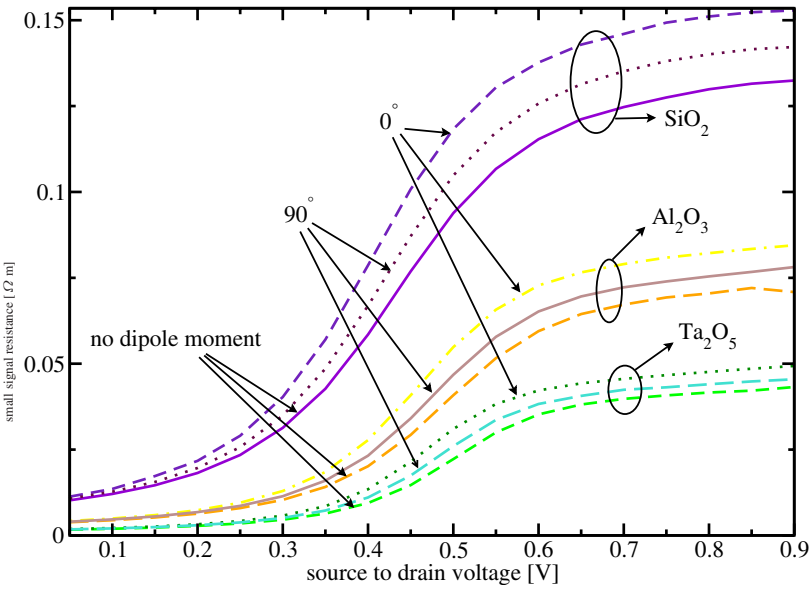

Fig. 10. Small signal resistance for SiO_2, Al_2O_3, and Ta_2O_5 calculated without dipole moment, angle $0°$ (perpendicular to surface), and angle $90°$ (parallel to surface) at bound state (biotin-streptavidin) for $10\,\mathrm{nm}$ average distance.

To increase the signal-to-noise ratio, the linker should have as little charge as possible. For example, in order to detect streptavidin, biotin is used as a binding agent. A biotin molecule is attached to the surface with a neutral linker. Streptavidin then binds to biotin thus forming a bound state. The charge difference between the unbound state of a biotin molecule alone, which is negatively charged with a single elementary charge and the bound state of biotin-streptavidin, which is negatively charged with five elementary charges, is large enough for detection. We also note that due to the tetrameric nature of streptavidin it has four sites to bind biotin as shown in Figure 11. Therefore, the linker binding biotin to the surface should be short enough in order to prevent binding several biotin molecules to a single molecule of streptavidin. If there is the freedom to choose attaching biotin or streptavidin via a linker to the surface, it will be better to use biotin. This will lead to a better signal to noise ratio because of the bigger change in surface charge, when the streptavidin charged with minus four elementary charges binds to biotin charged with minus one elementary charge. Additionally it offers the possibility to bind further proteins with biotin attached.

Fig. 11. Scheme of the tetrameric protein streptavidin and biotin.

5 Conclusions

The presented model shows a strong dependence on surface charges and indicates a detectable shift in the threshold voltage depending on their orientation related to the surface. The bound state (streptavidin-biotin) negatively charged with five elementary charges compared to the unbound state (biotin) negatively charged with one elementary charge leads to a reduced conductivity, when hybridization has taken place. Also the shift of the threshold voltage and output characteristics due to different molecule orientations ($0°$...perpendicular to surface, $90°$...lying flat on surface) can be seen. This demonstrates the usefulness of the simulation method for the design of efficient BioFETs.

Acknowledgements. This work was supported by the Austrian Science Fund FWF, Project P19997-N14.

References

1. Pirrung, M.C.: How to make a DNA chip. Angew. Chem. Int. Ed. 41, 1276–1289 (2002)
2. Shinwari, M.W., Deen, M.J., Landheer, D.: Study of the electrolyte-insulator-semiconductor field-effect transistor (EISFET) with applications in biosensor design. Microelectronics Reliability 47(12), 2025–2057 (2007)
3. Fritz, J., Cooper, E.B., Gaudet, S., Soger, P.K., Manalis, S.R.: Electronic detection of DNA by its intrinsic molecular charge. PNAS 99, 1412–1416 (2002)
4. Hahm, J., Lieber, C.M.: Direct ultrasensitive electrical detection of DNA and DNA sequence variations using nanowire nanosensors. Nano Letters 4(1), 51–54 (2004)
5. Gao, Z., Agarwal, A., Trigg, A., Singh, N., Fang, C., Tung, C., Fan, Y., Buddharaju, K., Kong, J.: Silicon nanowire arrays for label-free detection of DNA. Analytical Chemistry 79(9), 3291–3297 (2007)
6. Stern, E., Vacic, A., Reed, M.A.: Semiconducting nanowire field-effect transistor biomolecular sensors. IEEE Transactions on Electron Devices 55(11), 3119–3130 (2008)
7. Kim, S.N., Rusling, J.F., Papadimitrakopoulos, F.: Carbon nanotubes for electronic and electrochemical detection of biomolecules. Advanced Materials 19(20), 3214–3228 (2007)
8. Zheng, G., Patolsky, F., Cui, Y., Wang, W.U., Lieber, C.M.: Multiplexed electrical detection of cancer markers with nanowire sensor arrays. Nature Biotechnology 23(10), 1294–1301 (2005)
9. Im, H., Huang, X., Gu, B., Choi, Y.: A dielectric-modulated field-effect transistor for biosensing. Nature Nanotechnology 2(7), 430–434 (2007)
10. Cui, Y., Wei, Q., Park, H., Lieber, C.M.: Nanowire nanosensors for highly sensitive and selective detection of biological and chemical species. Science 293(5533), 1289–1292 (2001)
11. Gupta, S., Elias, M., Wen, X., Shapiro, J., Brillson, L.: Detection of clinical relevant levels of protein analyte under physiologic buffer using planar field effect transistors. Biosensors and Bioelectronics 24, 505–511 (2008)
12. Stern, E., Klemic, J., Routenberg, D., Wyrembak, P., Turner-Evans, D., Hamilton, A., LaVan, D., Fahmy, T., Reed, M.: Lable-free immunodetection with CMOS-compatible semiconducting nanowires. Nature Letters 445(1), 519–522 (2007)
13. Park, K.M., Lee, S.K., Sohn, Y.S., Choi, S.Y.: BioFET sensor for detection of albumin in urine. Electronic Letters 44(3) (January 2008)
14. Girard, A., Bendria, F., Sagazan, O.D., Harnois, M., Bihan, F.L., Salaün, A., Mohammed-Brahim, T., Brissot, P., Loréal, O.: Transferrin electronic detector for iron disease diagnostics. IEEE Sensors, 474–477 (October 2006)
15. Tang, T.W., Ieong, M.K.: Discretization of flux densities in device simulations using optimum artificial diffusivity. IEEE Transactions on Computer-Aided Design of Integrated Circuits and Systems 14(11), 1309–1315 (1995)
16. Selberherr, S.: Analysis and Simulation of Semiconductor Devices. Springer, Heidelberg (1984)
17. Poghossian, A., Cherstvy, A., Ingebrandt, S., Offenhäusser, A., Schöning, M.J.: Possibilities and limitations of label-free detection of DNA hybridization with field-effect-based devices. Sensors and Actuators, B: Chemical 111-112, 470–480 (2005)
18. Heitzinger, C., Kennell, R., Klimeck, G., Mauser, N., McLennan, M., Ringhofer, C.: Modeling and simulation of field-effect biosensors (BioFETs) and their deployment on the nanoHUB. J. Phys.: Conf. Ser. 107, 1–12 (2008)

19. Ringhofer, C., Heitzinger, C.: Multi-scale modeling and simulation of field-effect biosensors. ECS Transactions 14(1), 11–19 (2008)
20. Windbacher, T., Sverdlov, V., Selberherr, S., Heitzinger, C., Mauser, N., Ringhofer, C.: Simulation of field-effect biosensors (BioFETs). In: Proc. Simulation of Semiconductor Processes and Devices (SISPAD 2008), Hakone, Japan, September 2008, pp. 1–4 (2008)
21. Windbacher, T., Sverdlov, V., Selberherr, S., Heitzinger, C., Mauser, N., Ringhofer, C.: Simulation of field-effect biosensors (BioFETs) for biotin-streptavidin complexes. In: 29th International Conference on the Physics of Smeiconductors (ICPS 2008), Rio de Janeiro, Brasil (2008)
22. Protein data bank: (A resource for studying biological macromolecules), `http://www.pdb.org/`
23. Heitzinger, C., Klimeck, G.: Computational aspects of the three-dimensional feature-scale simulation of silicon-nanowire field-effect sensors for DNA detection. Journal of Computational Electronics 6, 387–390 (2007)
24. Landheer, D., Aers, G., McKinnon, W., Deen, M., Ranuárez, J.: Model for the field effect from layers of biological macromolecules on the gates of meta-oxide-semiconductor transistors. Journal of Applied Physics 98(4), 044701–1 –044701–15 (2005)
25. Stenkamp, R.E., Trong, I.L., Klumb, L., Stayton, P.S., Freitag, S.: Structural studies of the streptavidin binding loop. Protein Science 6(6), 1157–1166 (1997)
26. Deen, M.J., Shinwari, M.W., Ranuárez, J.C., Landheer, D.: Noise considerations in field-effect biosensors. Journal of Applied Physics 100(7), 074703–1 –074703–8 (2006)
27. Bousse, L.: The Chemical Sensitivity of Electrolyte/Insulator/Silicon Structures. Phd, Dissertation, Twente University of Technology, Enschede (1982)
28. Bousse, L., Mostarshed, S., Van Der Shoot, B., De Rooij, N.F., Gimmel, P., Gopel, W.: Zeta potential measurements of Ta_2O_5 and SiO_2 thin films. Journal of Colloid and Interface Science 147(1), 22–32 (1991)
29. Deen, M.J.: Highly sensitive, low-cost integrated biosensors. In: SBCCI 2007: 20th Symposium on Integrated Circuits and System Design, p. 1 (2007)
30. Oh, S.W., Moon, J.D., Lim, H.J., Park, S.Y., Kim, T., Park, J., Han, M.H., Snyder, M., Choi, E.Y.: Calixarene derivative as a tool for highly sensitive detection and oriented immobilization of proteins in a microarray format through noncovalent molecular interaction. FASEB Journal 19(10), 1335–1337 (2005)
31. Wacker, R., Schröder, H., Niemeyer, C.M.: Performance of antibody microarrays fabricated by either DNA-directed immobilization, direct spotting, or streptavidin-biotin attachment: A comparative study. Analytical Biochemistry 330(2), 281–287 (2004)
32. Kusnezow, W., Jacob, A., Walijew, A., Diehl, F., Hoheisel, J.D.: Antibody microarrays: An evaluation of production parameters. Proteomics 3(3), 254–264 (2003)
33. Peluso, P., Wilson, D.S., Do, D., Tran, H., Venkatasubbaiah, M., Quincy, D., Heidecker, B., Poindexter, K., Tolani, N., Phelan, M., Witte, K., Jung, L.S., Wagner, P., Nock, S.: Optimizing antibody immobilization strategies for the construction of protein microarrays. Analytical Biochemistry 312(2), 113–124 (2003)
34. Turková, J.: Oriented immobilization of biologically active proteins as a tool for revealing protein interactions and function. Journal of Chromatography B: Biomedical Sciences and Applications 722(1-2), 11–31 (1999)